Femtosecond Two-Photon Laser Photoelectron Microscopy

S. K. Sekatskii, S. V. Chekalin, A. L. Ivanov, Yu. A. Matveets, A. G. Stepanov, and V. S. Letokhov*

Institute of Spectroscopy, Russian Academy of Sciences, 142092 Troitsk, Moscow Region, Russia

Received: September 29, 1997; In Final Form: December 10, 1997

It is shown that high-resolution photoelectron images (with a resolution of up to 3 nm for ultrasharp silicon tips) can be obtained for practically all materials when irradiating tips made of these materials by pulses of the second harmonic of a femtosecond Ti:sapphire laser. In addition to the images, absolute values of the two-photon external photoelectric effect for these tips also can be measured using this method. The first experimental realization of this two-photon femtosecond laser projection photoelectron microscope is presented, and corresponding data for silicon, diamond, and calcium fluoride tips are analyzed.

Introduction

As is known, to solve numerous problems in surface physics, microelectronics, biophysics, and other fields requires application of research methods that possess an ultrahigh spatial resolution (up to a few nanometers) in combination with spectral (chemical) selectivity. Great expectations are associated with the laser photoelectron microscopy technique consisting in the detection with a high spatial resolution of electrons emitted by the sample under study upon laser irradiation. By appropriately selecting the laser irradiation conditions (with a view to implementing the selective photoionization of certain structures in the sample), one can not only observe the sample surface topography but also reveal the nature of the emission centers.[1,2]

The first experiments have recently been conducted in refs 3 and 4 that practically demonstrated the extensive capabilities of the laser photoionization microscopy technique (so far in its simplest lens-free, "projection" version): by irradiating the tips of single-crystal LiF needles containing F_2 centers with radiation from a CW argon laser, the authors have managed to attain a spatial resolution on the order of 30 nm and detect single F_2 centers, which are manifest as bright spots in the photoelectron images of the needle tips. The photoelectrons detected are due to the two-step photoionization of the F_2 centers by the argon laser radiation. Despite the moderate irradiation intensity (10^3−10^4 W/cm^2), the two-step ionization process has proven effective enough, this being explained by the existence in the F_2 centers of the ^3M triplet level with a sufficiently long lifetime. (See ref 3 for the details of the photoionization scheme used and ref 5 for the level structure of color centers in LiF crystals.)

Simple estimates show, however, that in the general case so low an irradiation intensity is obviously insufficient to implement any effective nonresonance two-photon ionization of solid-state samples, and obtaining photoelectron images requires applying much more powerful pulsed lasers. At the same time, neither the pulse energy nor the total power delivered to the sample should be high enough to give rise to problems associated with the optical breakdown of the sample, its thermal heating, and other effects occurring in strong light fields.

The analysis of the characteristics of the lasers existing today shows that an ideal source for observing resonance and nonresonance two-photon photoelectron images is femtosecond lasers with a very high (megahertz) pulse repetition frequency, specifically, the titanium sapphire femtosecond lasers that have recently gained wide recognition. By operating such a laser even without amplification of femtosecond pulses, one can easily obtain some 3−10 mW of average power in the second-harmonic radiation at a wavelength of 410 nm, which corresponds to the energy of a quantum $h\nu = 3.02$ eV. This power, as well as the energy of a single pulse, is too low to cause any of the problems mentioned above. At the same time, given the parameters of our laser—a pulse duration of $\tau = 40$ fs, a pulse repetition frequency of $f = 82$ MHz, and a laser beam spot area of 0.1−0.01 mm^2—such a power corresponds to an intensity of $I = 10^6$ to 3×10^7 W/cm^2, which proves quite sufficient for the detection of bright photoelectron images of a wide range of samples. Certainly, the same technique can be used for obtaining photoelectron images of single molecules in matrixes, including the low-temperature case.

In the present paper, we report on the experimental implementation of such a femtosecond photoelectron microscope and present the results obtained with its aid in investigating samples made of silicon, diamond, and calcium fluoride. Such semiconductive and dielectric samples were deliberately chosen by us for the first pilot experiments: practically for all metals the work function value is less than the two-laser quanta energy of 6.04 eV, and the possibility of observation of bright photoelectron images of metal tips is obvious. The possibility is also analyzed of using this microscope for taking *quantitative* measurements of the two-photon external photoelectric effect in silicon, diamond, and calcium fluoride.

Experimental Section

Laser Photoelectron Microscope. A schematic diagram of a photoelectron projection microscope is presented in Figure 1. The sample under study is a sharp-pointed needle with a tip radius of curvature equal to r, which is held fast in a special holder at a distance of $L = 10$ cm from the detector: a microchannel plate (MCP) and phosphorescent screen assembly (Hamamatsu Photonics K. K., Japan). A voltage U in the range 0−4 kV is applied to the sample (the microchannel plate input is grounded), and if this voltage is high enough, there takes place an effective field (tunnel) emission of electrons from the needle tip. The radial electric field existent in the vicinity of the tip directs the electrons emitted onto the detector to form

S1089-5639(97)03153-8 CCC: $15.00
Published on Web 02/26/1998

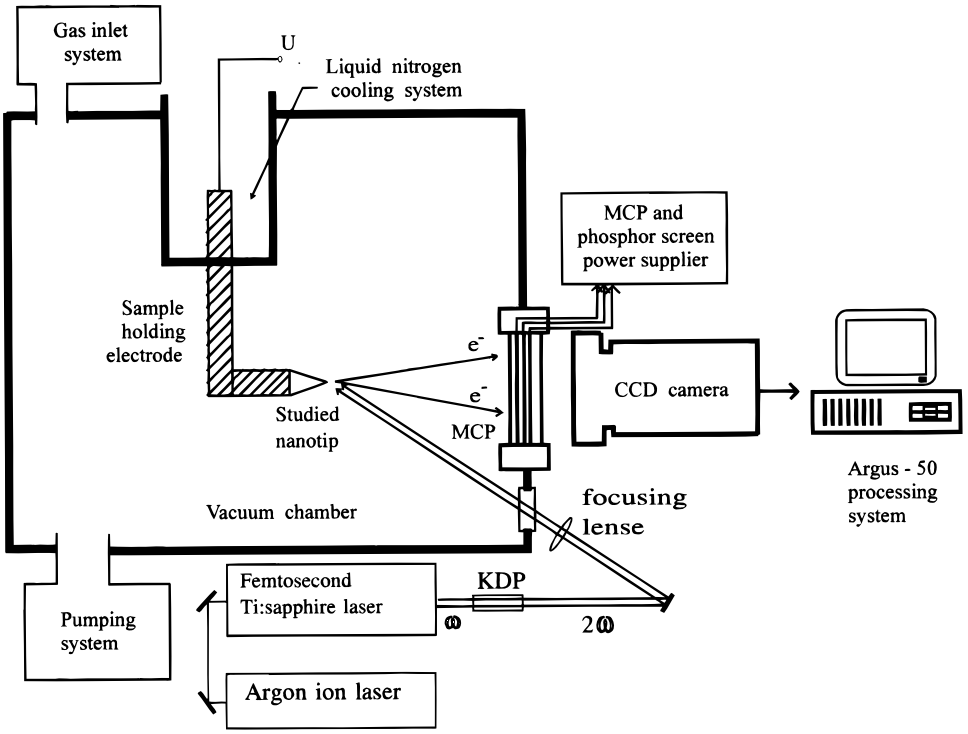

Figure 1. Schematic of the laser photoelectron projection microscope.

on its screen a magnified image of the tip. The magnification M is equal to $M = L/\gamma r$, where γ is a numerical factor ranging between 1.5 and 2 (see any monograph on the field electron/ion microscopy techniques, for example ref 6). When studying photoelectron and not field-emission images of needle tips, the needle potential is lowered to a level at which the tunnel emission of electrons from the tip is zero, their emission being due solely to the photoemissive effect in the needle material caused by the second-harmonic radiation of the Ti:sapphire laser used (the laser parameters have been indicated in the Introduction). As in the case of field emission, the electric field in the vicinity of the tip directs the photoelectrons emitted onto the detector to form, with the same magnification, a photoelectron, and not a field-emission image of the tip.

The spatial resolution of the microscope is limited because of the presence of electrons emitted of a certain average nonzero transverse energy E_0 and is given by[6]

$$d \approx 4\gamma r\sqrt{E_0/eU} \qquad (1)$$

The use of this formula for $E_0 = 0.5$ eV, $r = 250$ nm, and $U =$ 1kV yields $d \cong 30$ nm. When investigating needle tips with smaller radii of curvature, the spatial resolution of the microscope can be much higher, can approach the theoretical limit set by the Heisenberg uncertainty principle (the more accurate the determination of the emitting center coordinate, the greater should be the spread arising in the momentum of the emitted electrons), and is typically equal to 1−2 nm.

The same microscope, except the laser part, was used earlier to study LiF:F_2 samples in refs 3 and 4, and so the readers interested in its more detailed description are referred to these works.

Samples. The samples studied were ultrasharp silicon needles (radius of curvature less than 25 nm) prepared at the Institute of Crystallography of the Russian Academy of Sciences in Moscow and the same needles coated with a comparatively thick layer of diamond or calcium fluoride. The sample preparation procedure was briefly as follows.

High-conductivity n-type single-crystal silicon whiskers were grown on one end of a (111) Si rod $1 \times 1 \times 100$ mm^3 in size. The growth end face of the rod was polished and etched with a HF−HNO_3 solution. The size of the rod face after the pregrowth preparation was some 0.5×0.5 mm^2. The as-grown whiskers were first sharpened by wet etching. Thereafter they were subjected to repeated thermal oxidation with subsequent HF-etch oxide removal. The prepared whisker tips were 100 μm high, their radius of curvature being less than 25 nm. Further details on the vapor−liquid−solid growth technique and sharpening procedure can be found in ref 7. The prepared silicon emitter arrays were coated with diamond by the hot filament CVD vapor deposition technique,[8] the radius of curvature of the diamond coating ranging between 250 and 350 nm in the samples studied.

CaF_2 films were grown on Si whiskers by the molecular beam epitaxy (MBE) technique. The base pressure in the growth chamber amounted to 0.5×10^{-11} Torr, and CaF_2 containing samarium in the necessary concentration was evaporated from a Knudsen cell. The temperature of the Si whiskers in the course of the MBE growth process was around 500−600 °C. The thickness of the CaF_2 coating was in the range 50−100 nm. Further details on growth of the CaF_2 coating on Si whiskers can be found in ref 9.

Photoelectron Images of Needle Tips and Their Analysis

Diamond-Coated Silicon Nanotips. We will start the discussion of the laser photoelectron images of the tips for the case of diamond-coated silicon tips. The importance of such investigations stems from an understanding of the reasons of effective field emission from diamond and diamond-like materials (see, for example, papers 10−12 and references therein). The low field emission threshold (up to 3 V/μm) and high intensity and stability of the emission current observed with emitters fabricated from diamonds, diamond films, and diamond coatings on ultrasharp silicon needles have drawn much attention to "diamond materials" as promising new materials for vacuum

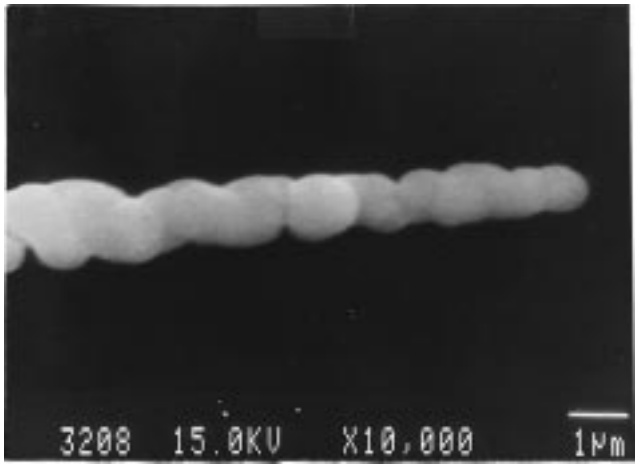

Figure 2. Scanning electron microscope image of a typical diamond-coated silicon nanotip.

electronics, primarily for cold-cathode and field-emission-display technologies. Despite the fact that the emission characteristics of such materials have already been investigated in numerous works, the mechanisms and causes of the effective, low-threshold emission from diamonds, diamond films, and diamond coatings still remain unclear; see, for example, the discussion of various possible mechanisms (conduction-band emission from a negative-electron-affinity (NEA) diamond surface, valence-band emission from nanoprotrusions, hot electron emission, the possible role of defects or nondiamond inclusions, and so on) in refs 13 and 14 and references therein.

To elucidate these questions, it seems very important to study the emissive properties of such structures with a high spatial resolution and analyze the correlation between these properties and various diamond characteristics (crystallographic orientation of single crystals, local concentration of defects, etc.). For these reasons it seems very interesting to investigate diamond-related emitters using field emission microscopy (FEM) methods, which are capable of nanometer spatial resolution.[6] Additional and rather interesting information about the object under study can be collected using laser photoelectron projection microscopy of the tips based on femtosecond Ti:sapphire lasers, and the comparison of both types of images is of special importance.

The scanning electron microscope image of one of the nanotips studied is presented in Figure 2, while the laser photoelectron image of this tip is presented in Figure 3a. The tip potential was insufficient to cause field emission from the nanotip, the photoelectric current being found to be practically independent of tip potential and to depend on the radiation intensity in a quadratic fashion, as shown in Figure 4. These experimental observations unambiguously point to the fact that the photoelectron images of the tips are due to the nonresonance two-photon photoemission from the diamond coatings under the effect of femtosecond laser pulses with a quantum energy of 3.02 eV (and not to the, for instance, laser-assisted field emission from the diamond, because in that case the dependence of photocurrent on the tip potential would be much sharper; compare with data presented, for example, in ref 15). Such a conclusion corresponds quite well to the previous works devoted to external photoelectric effect from the diamond, where a photoemission threshold value of 5.5 eV was determined,[16] as well as to the following known data: the band gap E_g value of the diamond is equal to 5.5 eV and a negative electron affinity χ value for some crystallographic planes of diamond was reported.[17,18] It is known also that an electron affinity value for the diamond depends critically on the nature of crystal-

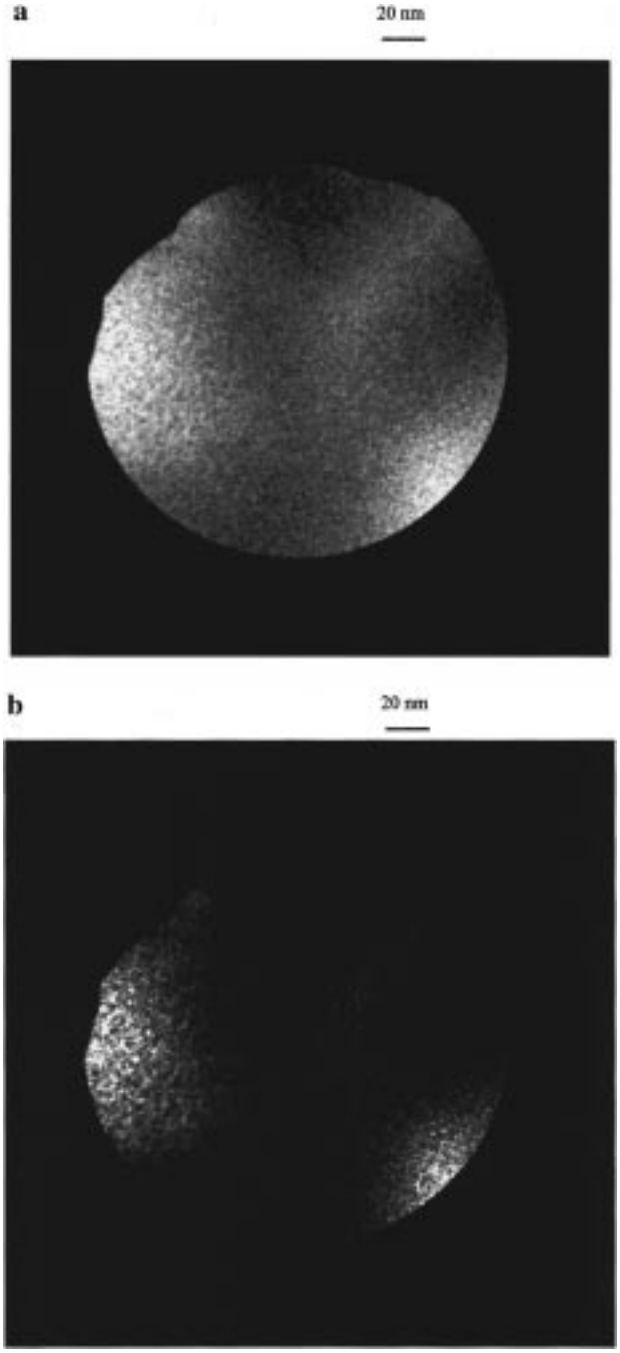

Figure 3. Emission images of a diamond-coated silicon nanotip with a radius of curvature of 350 nm: (a) laser photoelectron image, $U_{tip} = 1.6$ kV, $I \cong 3 \times 10^6$ W/cm^2; (b) field-emission image, $U_{tip} = 2.4$ kV.

lographic plane and the concrete conditions on this plane and can be varied in a rather broad range, at least from -2.2 to $+0.8$ eV.[18] The relation $2h\nu > E_g + \chi$ should take place to observe an effective photoemission from dielectrics or semiconductors, and thus, some crystallographic planes formed at the tip of a Si/diamond needle must contribute to the photocurrent due to the irradiation of the tip by the second harmonic of the Ti:sapphire laser and can be visualized in the photoelectron images of the tip, while the other planes make no contribution to the photocurrent and must be manifest as dark spots in the images. In our view, it is exactly in this way that one should interpret the photoelectron images of diamond coatings, which feature distinct light and dark spots (emitting and nonemitting regions) typically from 30 to 100 nm across; it is known from FEM experience that at the tips of metal and

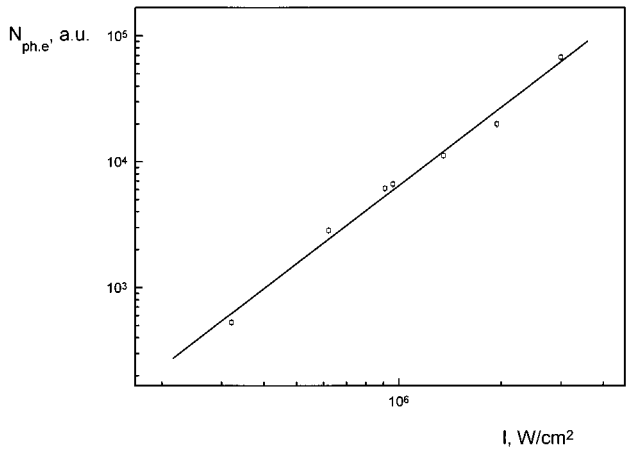

Figure 4. Photoelectric current $N_{ph.el.}$ as a function of the radiation intensity I of the second harmonic of the Ti:sapphire laser irradiating the diamond-coated tip.

semiconductor needles there exist both atomically ordered regions differing in crystallographic orientation and atomically disordered regions with a typical size on the order of tens to one hundred nanometers.[6]

A field-emission image of the same diamond-coated nanotip is presented in Figure 3b for comparison. This image was registered at a higher tip potential and without laser irradiation; it is clear that it is very similar to the image presented in Figure 3a and differs from it practically only in higher contrast. Such a similarity was found to exist with all the tips studied, and this observation is, in our view, the main result of the experiments devoted to diamond-coated-nanotip investigations. Certainly, this similarity reflects first of all the fact that the same local characteristics, such as work function and/or electron affinity, are important for both effective field emission and external photoelectric effect. At the same time we would like to note that such a similarity is not a trivial fact (essentially poorer similarity was observed, for instance, for calcium fluoride coatings; see below), and, what is very important, it clearly demonstrates that exactly the images of the nanotips and nothing else are registered by laser photoelectron projection microscopy technique.

In this paper we will not discuss the observed laser photoelectron and field-emission images of diamond-coated silicon nanotips in further detail; this material is more interesting for specialists of field emission phenomena and will be published elsewhere. Here we would like to pay attention to the fact that the method considered enables one also to determine rather easily and with high accuracy an absolute value of the two-photon photoelectric effect yield coefficient β_2 for the materials under study. We define β_2 as a coefficient that connects the pulsed two-photon photoemission intensity $N_{ph.e.,\ pulsed}$ (expressed in photoelectrons/cm^2 s) with the pulsed laser light intensity I (expressed in photons/cm^2 s): $N_{ph.e.,pulsed} = \beta_2 I^2$.

Indeed, an area from which photoelectrons are collected, S, is determined by the geometry of the microscope (tip−detector distance $L = 10$ cm and working region of the MCP diameter $d = 32$ mm) and can easily be calculated as $S = \xi\pi/4(\chi dr/L)^2 \cong 0.3r^2$. This relation merely reflects the fact that such an area is equal to the size of the working area of MCP d divided by the magnification coefficient M; the factor ξ is close to unity and takes into account the fact that the surface of the tip apex is not flat but hemispherical (from elementary geometry it is easy to calculate that for our experimental conditions $\xi \cong 1.03$ and thus can be neglected); spatial variations of M can be neglected.[6] Despite the small size of this emitting area, it nevertheless is generally larger than the typical photoelectron escape depth l_{esc} value for the materials studied; the latter usually ranges from 0.1 to 10 nm.[19] For this reason, the results obtained can be correctly compared with the results obtained using "classic" experimental approaches based on irradiation of flat surfaces with the focused laser beam (see, for example, refs 20−22 and references therein; calcium fluoride is an exception, where the reciprocal relation $l_{esc} \gg r$ takes place; see below).

The laser irradiation intensity I also can easily be measured with a high accuracy because strong focusing is not used in the experiments described, and thus it is not a problem to measure the laser light spot size in the area of an apex. Working in a photoelectron pulses counting mode and assuming 100% efficiency for an MCP-based detector (it is not a problem to introduce the corresponding correction coefficient, if necessary), one can easily measure the flux of photoelectrons per second, which should be equal to

$$N_{ph.e.} = \beta_2 I^2 S f\tau = \beta_2 I_0 2S/(h\nu)^2 f\tau \qquad (2)$$

For simplicity we introduced here an equivalent "continuous working" laser light intensity I_0 (expressed in W/cm^2 s): $I = I_0/h\nu f\tau$ (f and τ are laser pulse repetition rate and duration, which have been defined in the Introduction). Thus, when measuring the $N_{ph.e.}$ value, one can easily calculate the β_2 value, for our experimental conditions:

$$\beta = N_{ph.e.}(h\nu)^2 f\tau/I_0 2S = 7.65 \times 10^{-43} N_{ph.e.}/I_0{}^2 S \qquad (3)$$

Using formula 3 we can determine for the diamond the following coefficient of two-photon external photoelectric effect under the action of light with the wavelength of 410 nm: $\beta_2 = 1.9 \times 10^{-33}$ cm^2 s (averaged); for the brightest regions in Figure 3a coefficient β_2 is at least 7-fold greater: $\beta_2 = 1.3 \times 10^{-32}$ cm^2 s.

Coefficient β_2 is in the same range as other known values of two-photon photoelectric effect yield coefficients from semiconductors and dielectrics.[20−22] Our approach has an additional advantage in comparison with the other "classic" methods of measuring an external photoelectric effect yield, because we measure not only the *averaged* value of the β_2 coefficient but its *local* values (with a spatial resolution on the order of 30−40 nm or even better) as well. It should be noted that we neglected the reflection of light from the surface studied and the variation of the angle of the light incidence when calculating the β_2 value, but such a neglect is typical for all methods of two-photon external photoelectric effect yield coefficient measurements.[20−22]

Calcium Fluoride-Coated Silicon Nanotips. Photoemission intensity for the case of calcium fluoride-coated silicon nanotips was much weaker than for the diamond-coated silicon nanotip case, and any material structure in the photoelectron images was absent. The photocurrent also reveals a quadratic dependence on irradiation intensity and was attributed to the laser two-photon external photoelectric effect.

Field-emission images of these nanotips look like a sufficiently usual set of dark and bright spots and were more or less similar to that presented in Figure 3b for diamond-coated tips. No material correlation between laser photoelectron and field-emission images has been revealed.

The external photoelectric effect threshold for calcium fluoride is very high and ranges 8−9 eV,[23] and thus such a threshold is essentially higher than the energy of two quanta of laser radiation used. But it is well-established that some

"residual" photoemission exists also in the "below the threshold" region of irradiation quanta energy. Such photoemission is due to the photoionization of different defects and/or impurities in the samples and was reported earlier for many materials. For example, in ref 21 for the irradiation of KCl, KI, and CsI by the second harmonic of a ruby laser radiation two-photon photoelectric effect yield a coefficient β_2 that exceeds the value of 10^{-32} cm^2 s was reported.

We believe that the photoelectron images of calcium fluoride-coated tips observed by us are due to the same effect of photoionization of impurities and/or defects. The absence of the clear structure in the images can be associated with the anomalously high photoelectron escape depth l_{esc} for the calcium fluoride: in ref 24 it was reported that such a depth can attain the value of 260 nm. (High emissive characteristics of Si:CaF_2 nanotips[15] are also consistent with such rather high electron escape depth values.) Thus, practically all defects containing a calcium fluoride coating with a thickness of 50−100 nm can contribute to the observed photoelectron images. This circumstance as well as the scattering of photoelectrons inside a coating leads to the "averaging" of images and is the reason for the absence of the structure in the images. We did not make quantitative measurements of the two-photon photoelectric effect yield for CaF_2 coatings because in this case the relation $r \gg l_{esc}$ did not take place and such measurements do not make sense.

Ultrasharp Silicon Tips. A laser photoelectron image of an ultrasharp silicon tip is presented in Figure 5a; for comparison the field-emission image of the same tip is presented in Figure 5b. Well-developed structure is absent in both images, and such an absence of clear structure was characteristic for all silicon tips studied. We believe that this is due to the "amorphous" character of a tip surface. Such a suggestion is consistent with the impossibility of observing high-quality (high-resolution) field ion microscope images of these ultrasharp silicon tips and is not surprising because it is known that to obtain a well-developed crystal structure of a silicon tip, it is necessary to process it with careful thermal annealing and field evaporation in UHV condition.[6,25]

At the same time for one of the silicon tips studied we have observed a clear difference between laser photoelectron and field emission images, which is illustrated in Figures 5a,b. It is seen that an additional bright spot, which is absent in the field-emission image, is present in the photoelectron image. In all probability this spot is due to the presence of some effectively light-absorbing impurity (defect) close to the silicon tip surface (reported photoelectron escape depth for the silicon is estimated to be 1.2 nm[26]), but in this paper we would not like to dwell on a detailed interpretation, which will be published elsewhere. Note that different types of defects in silicon have been extensively studied by "classic" methods of semiconductor physics earlier (see, for instance, refs 27, 28 and papers cited therein), and their observation with an ultrahigh spatial resolution seems rather important for us.

Our purpose here is to underline that Figure 5a is, to the best of our knowledge, a demonstration of the best achieved spatial resolution for a photoelectron microscope. For the radius of curvature of a tip $r = 20$ nm, tip potential 1 kV, and average transverse kinetic energy of an emitted electron 0.75 eV (this is half of the difference between the energy of two-laser quanta and work function of a silicon, which is equal to 4.5 eV[29]) an application of relation 1 gives the value $d = 3$ nm for the spatial resolution, and it is illustrated in Figure 5a.

The observed photocurrent, just as for the diamond and the calcium fluoride cases, depended quadratically on the irradiation intensity I. The absolute value of a coefficient of two-photon external photoelectric effect yield β_2 (for the wavelength of 410 nm, averaged) was measured to be 1.5×10^{-32} cm^2 s. Such a value corresponds well with the known value of an analogous coefficient for the wavelength of 355 nm: $\beta_2 = 2.5 \times 10^{-32}$ cm^2 s.[22]

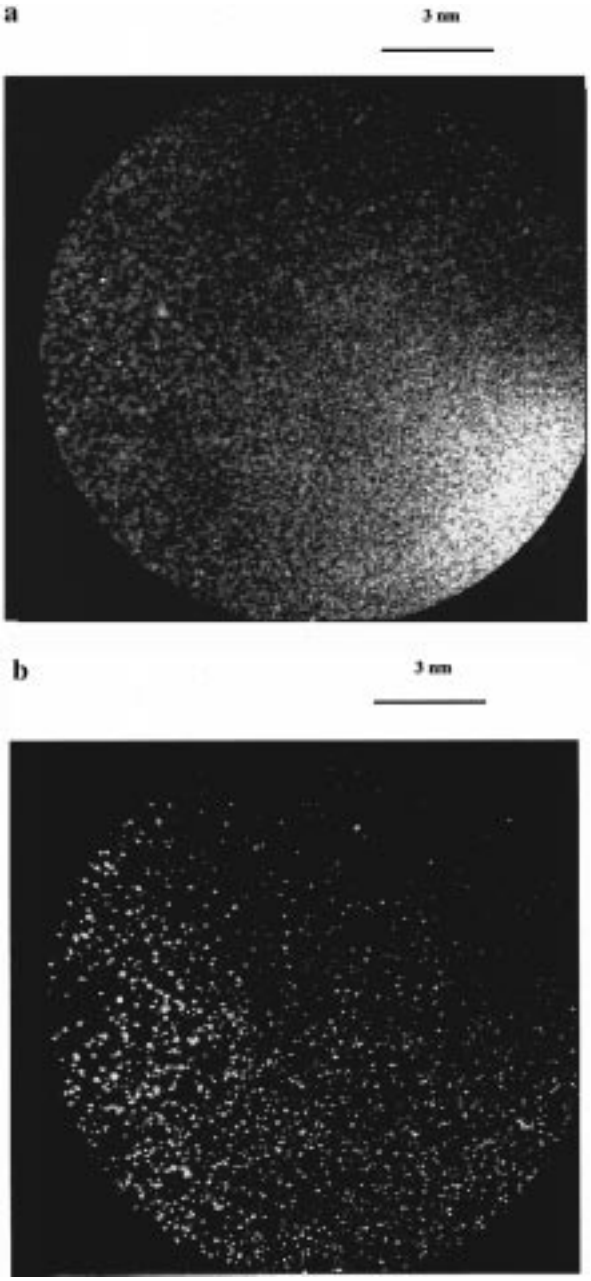

Figure 5. Emission images of an ultrasharp silicon nanotip with a radius of curvature of 20 nm: (a) laser photoelectron image, $U_{tip} = 1.0$ kV, $I \cong 3 \times 10^6$ W/cm^2; (b) field-emission image, $U_{tip} = 1.5$ kV.

Conclusions

The data presented by us convincingly demonstrate the extensive possibilities offered by femtosecond lasers with a megahertz-high pulse repetition frequency for the laser photoelectron projection microscopy technique. A photoelectron microscope equipped with such a laser becomes a universal tool fit to study practically any metal, semiconductor, or dielectric samples. From the circumstance that the noise level of the detector (microchannel plate + phosphorescent screen) used in the microscope is clearly less than one count per second, it

follows (formula 3 at $I_0 = 10$ W/cm^2) that quite informative photoelectron images can be obtained for materials whose two-photon photoemissive effect yield coefficient β_2 at a wavelength of 410 nm is more than $\sim 10^{-33}$ cm^2 s at $r = 50$ nm or more than $\sim 6\ 10^{-33}$ W/cm^2 at $r = 20$ nm. Both our experimental results and the results of numerous experimental works devoted to research into the multiphoton laser photoelectric effect in solids[20−22] point to the fact that the β_2 coefficient is more than 10^{-33} cm^2 s even for those dielectrics in which the energy of two quanta of the laser radiation used is less than the band gap (CaF_2, KCl, glass, etc.), so that photoelectron images can practically be obtained for any samples.

Separately we would like to mention that the possibilities of using the femtosecond Ti:sapphire lasers certainly are not limited to the above considered case of lens-free projection photoelectron microscopy. The same consideration is valid for the case of "classic" photoelectron microscopes as well (we mean photoelectron microscopes equipped with magnetic or electrostatic lenses capable of forming a high-resolution image of a *flat* sample; for a review see, for example, ref 19). The spatial resolution of the modern photoelectron microscope attains 40 nm;[30] thus using formula 2 with the values of $I_0 = 10$ W/cm^2 and $\beta_2 = 10^{-32}$ cm^2 s, one can see that it is possible to obtain $\sim$20 photoelectrons per second from a resolution-limited spot when applying a Ti:sapphire femtosecond laser as a photoelectron source. Such photoelectron flux should be sufficient to obtain a bright photoelectron image even when one uses high collimation of the photoelectron beam to improve the spatial resolution. Note also that due to the high repetition rate of femtosecond Ti:sapphire laser pulses, a bright image can be obtained even when one gets essentially less than one photoelectron per laser pulse. This also helps to avoid the problems associated with the electrostatic repulsion of the emitted photoelectrons.[19]

The first experiments with the laser projection photoelectron microscope enable one to observe the spatial distribution of F_2 color centers on LiF tips[3,4] and single defects on silicon (this paper) and calcium fluoride (to be published) tips. There can be no doubt that such investigations will prove useful in the analysis of nanostructures in materials, local work function values, defect concentrations, and so on. We believe that this two-photon femtosecond laser projection microscopy will be used also for the direct visualization of biomolecules "trapped" inside specially selected matrices (such as paraffin or analogues), as it was discussed earlier, for instance in ref 31. Sharp tips can be prepared out of such "solid solutions"; low temperature and ultrashort light pulses are necessary for the effective excitation of dissolved molecules (because energy transfer to the environment probably will be too effective).

The principal possibilities to obtain also an ultrahigh temporal resolution when using femtosecond laser pulses should also be mentioned, but their detailed discussion lies far beyond the scope of the present paper.

For the conclusion we would like specifically to emphasize once more the importance and convenience of such photoelectron microscopic measurements in gathering quantitative data on the single- or multiple-photon photoelectric effect, for what takes place here is the simultaneous and "automatic" measurement of both the photocurrent and the area of the emitting region. If necessary, the sensitivity of such measurements can be improved by going over to the recording of low-magnification photoelectron images, when the laser is focused not exactly onto the apex of the tip but into a spot some small distance from the apex[32] when photoelectrons are collected from a much greater area *S*.

Acknowledgment. This work was partially supported financially by The Russian Fundamental Research Foundation, the U.S. Department of Defense, and CRDF Grant RP2-154. The authors are thankful to Hamamatsu Photonics K. K., Japan, for the provision of the necessary experimental equipment, and also to V. V. Zhirnov and E. I. Givargizov for the provision of silicon and diamond-coated silicon tips and N. S. Sokolov and J. C. Alvaretz for the preparation of calcium fluoride coatings.

References and Notes

(1) (a) Letokhov, V. S. *Kvantovaya Elektron.* **1975**, *2*, 930 (in Russian). (b) Letokhov, V. S. *Phys. Lett. A* **1975**, *51*, 231.
(2) Letokhov, V. S.; Sekatskii, S. K. *Appl. Phys. B* **1992**, 55, 177.
(3) Konopsky, V. N.; Sekatskii, S. K.; Letokhov, V. S. *Opt. Commun.* **1996**, *132*, 251.
(4) Sekatskii, S. K.; Letokhov, V. S. *JETP Lett.* **1997**, *65*, 465.
(5) Nepomnyashchikh, A. I.; Radzhabov, E. A.; Egranov, A. V. *Color Centers and Luminescence in LiF Crystals;* Nauka: Novosibirsk, 1984 (in Russian).
(6) Tsong, T. T. *Atom-Probe Field Ion Microscopy;* Cambridge University Press: Cambridge, 1990.
(7) Givargizov, E. I. *J. Vac. Sci. Technol., B* **1993**, *11*, 449.
(8) Givargizov, E. I.; Zhirnov, V. V.; Kuznetsov, A. V.; Plekhanov, P. S. *Mater. Lett.* **1993**, *18*, 61.
(9) Sokolov, N. S.; Alvaretz, J. C.; Yakovlev, N. L. *Appl. Surf. Sci.* **1992**, *60*/*61*, 421.
(10) Wang, C.; Garcia, A.; Ingram, D. C.; Lake, M.; Kordesh, M. E. *Electron. Lett.* **1991**, *27*, 1459.
(11) Xu, N. S.; Tzeng, Y.; Latharn, R. V. *J. Phys. D* **1993**, *26*, 1778.
(12) Givargizov, E. I.; Zhirnov, V. V.; Stepanova, A. N.; Rakova, E. V.; Kiselev, A. N.; Plekhanov, P. S. *Appl. Surf. Sci.* **1994**, *87*/*88*, 24.
(13) Huang, Z.-H.; Cutler, P. H.; Miskovsky, N. M.; Sullivan, T. E. *Appl. Phys. Lett.* **1994**, *65*, 2562.
(14) Zhirnov, V. V. *J. Phys. IV* **1996**, C5−6, 107.
(15) Konopsky, V. N.; Zhirnov, V. V.; Sokolov, N. S.; et al. *J. Phys. IV* **1996**, *C5*−*6*, 129.
(16) Bandis, C.; Pate, B. B. *Phys. Rev. Lett.* **1995**, 74, 777.
(17) Himpsel, F. J.; Knapp, J. A.; VanVechten, J. A.; Eastmann, D. E. *Phys. Rev. B* **1979**, *20*, 624.
(18) van der Weide, J.; Zhang, Z.; Baumann, P. K.; et al. *Phys. Rev. B* **1994**, *50*, 5803.
(19) Griffith, O. H.; Rempfer, G. F. *Adv. Opt. Electron Microsc.* **1987**, *10*, 269.
(20) Lazneva, E. F. *Laser Desorption;* Leningrad State University Publ. House: Leningrad, 1990 (in Russian).
(21) Logothetis, E. M.; Hartman, P. L. *Phys. Rev.* **1969**, *187*, 460.
(22) Leung, T. L. F.; van Driel, H. M. *Appl. Phys. Lett.* **1984**, *45*, 683.
(23) Pole, R. T.; Szajman, J.; Leckey, R. C. J.; et al. *Phys. Rev. B* **1975**, *12*, 5872.
(24) Quiniou, B.; Schwarz, W.; Wu, Z.; et al. *Appl. Phys. Lett.* **1992**, *60*, 183.
(25) Liu, H. M.; Tsong, T. T. *J. Appl. Phys.* **1987**, *63*, 1532.
(26) Sebenne, C.; Bolmont, D.; Guichar, G.; Balkanski, M. *Phys. Rev. B* **1975**, *12*, 3280.
(27) Walker, J. W.; Sah, S. T. *Phys. Rev. B* **1973**, *7*, 4587.
(28) Irmscher, K.; Klose, H.; Maass, K. *Phys. Status Solidi A* **1983**, *75*, K25.
(29) Broudy, R. M. *Phys. Rev. B* **1970**, *1*, 3430.
(30) Staib Instrumente GmbH, Langenbach, Germany, Model PEEM-350.
(31) Letokhov, V. S. In *Laser Spectroscopy IX*; Feld, M. S., Thomas, J. E., Mooradian, A., Eds.; Academic Press: New York, 1989; p 494.
(32) Sekatskii, S. K. *Sov. Phys. JETP* **1997**, *112*, 690.